

Introduction

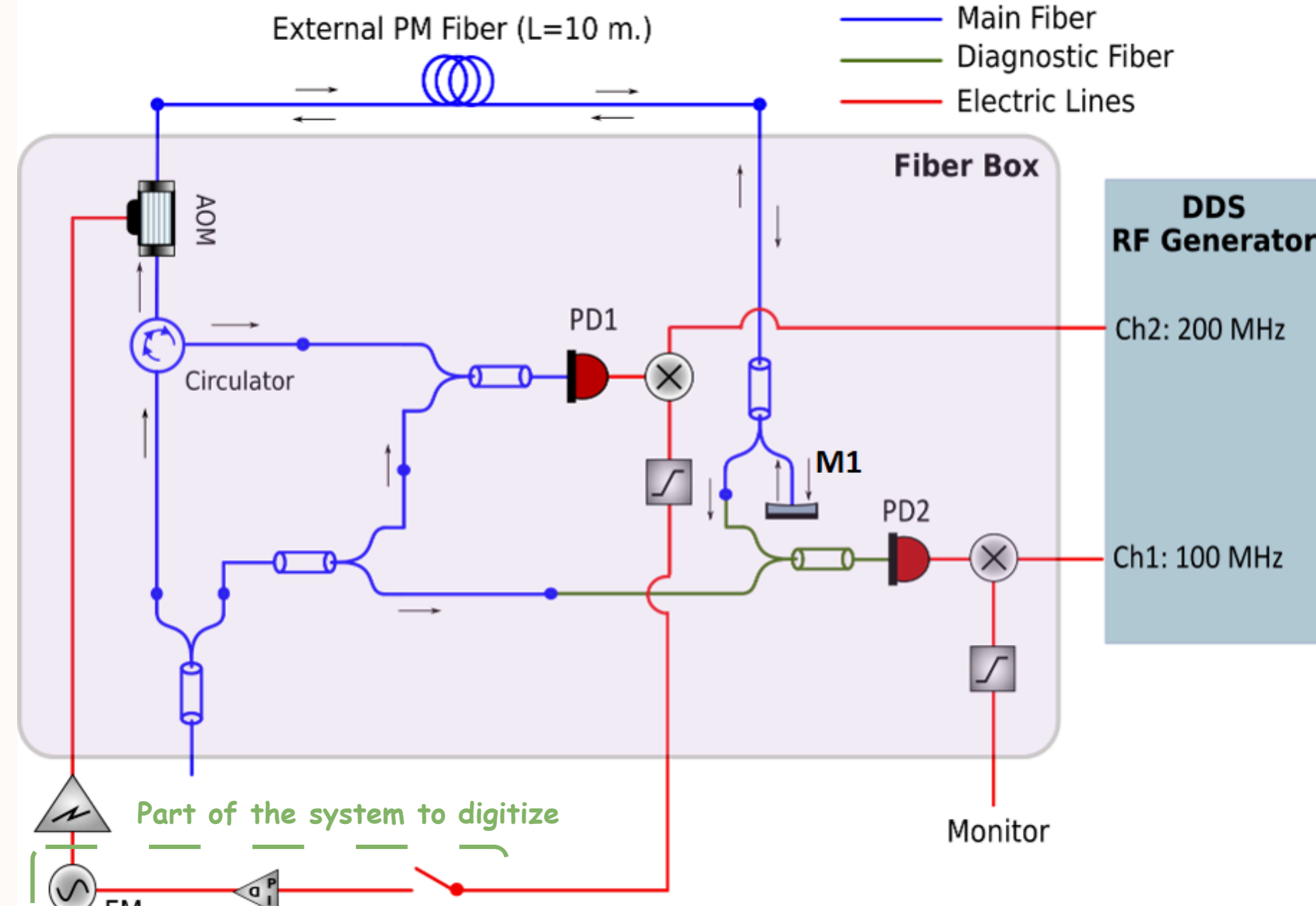
The “all in fiber” phase noise cancellation loop demonstrator makes use of some pigtailed mirrors, beam splitters and photodetectors to sense phase deviations, and an acousto-optic modulator (AOM) to apply proper frequency shift to the reference beam of VIRGO detector’s squeezer. This compensates, to a certain extent, environmental factors affecting the phase of light along its path. The setup used to employ a bench-top analog RF generator with external frequency modulation capability to drive the AOM. Such instrument has recently been replaced with a direct digital synthesizer, improving system integration and reconfigurability, with the substantial advantage of an overall lower phase noise profile of the modulated RF tone. Moreover, the settling time for frequency steering has also been reduced by almost an order of magnitude with respect to the original circuit, allowing to extend the noise reduction bandwidth to 100 kHz. The loop compensation, once put in place with an analog PID module and tuned with Ziegler-Nichols procedure, has been transposed to the digital domain by “emulation” using Tustin’s method.

Noise reduction loop working principle

A fraction of the light arriving at the experimental port is reflected back by the mirror M1, accumulating twice the phase noise ϕ_n of the external fibre (of length $L = 10$ m). Subsequently, by means of a circulator, this beam is diverted to the PD1 photodiode where it meets the primary beam, generating a beat note at twice the AOM driving frequency ($\Omega = 100$ MHz). Demodulating this signal at $2\phi_n$ yields to an estimate of $2\phi_n$. This error signal is compensated by closing the loop acting on the FM channel of the AOM’s RF driver. The loop requires the use of the following components:

- ◇ an acousto-optical modulator to shift frequency & phase of the light beam according to the driving signal;
- ◇ power splitters & combiners;
- ◇ VIRGO Quad-DDS, for reference tones generation;
- ◇ photodetectors, (integrated) analog mixers and RF low-pass filters to extract the observed frequency/phase deviation w.r.t. reference.

An HP8656B synthesized signal generator (synchronized with a 10 MHz Quad-DDS signal) drives the AOM, set in external frequency modulation mode, with an output power of -10 dBm, then amplified to meet the 30 dBm requirement of the AOM. A SRS SIM960 analog PID controller module is also included to meet the requested ~ 20 kHz loop bandwidth.



DDS-based FM modulation

Generation of any arbitrary waveform is possible with a DAC and a memory containing the samples evolution. In a DDS, a lookup table is used to store the values of a sine wave, and tone modulation is obtained by jumping between variably spaced samples. Rigid translation of LUT index scan then allows the phase to be altered. AD9914 features:

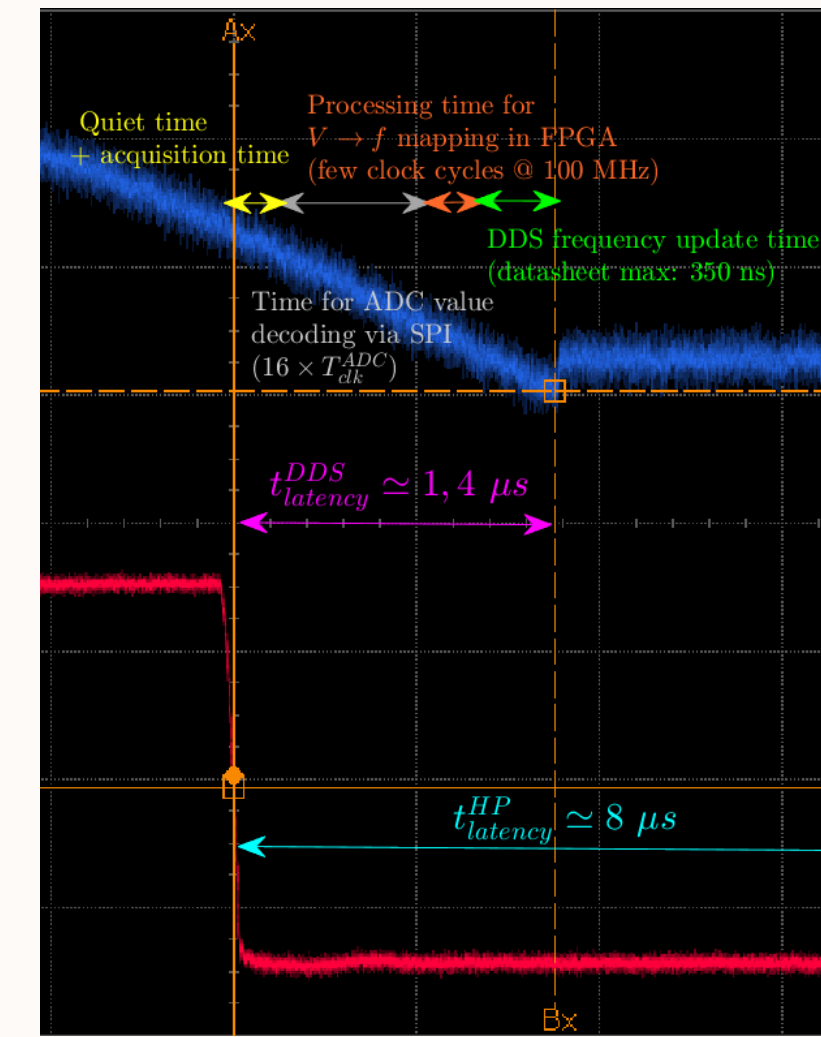
- many operating modes, upon which ‘direct frequency control’ via 32-bit parallel bus ($df = f_{clk} \times 2^{-32}$)
- 17-bit LUT, 32-bit phase accumulator, 12-bit output DAC
- $f_{clk} = 2.4$ GHz, starting from 200 MHz Wenzel OXCO



Integrated phase noise of RF source: 20 mrad \rightarrow 1 mrad.
 \hookrightarrow ADC’s quantization noise is the dominant factor!

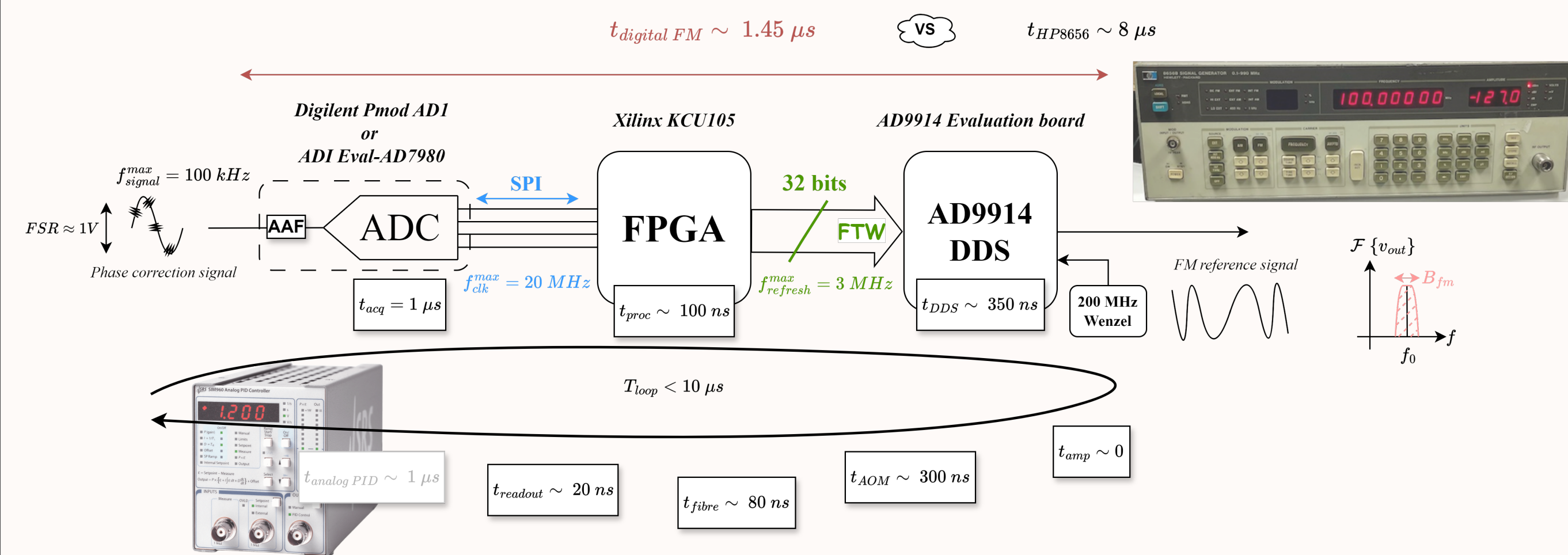
Control firmware

1. SPI master for ADC, providing clock and chip select signals with proper timing
2. Pre-processing averager block for noise removal
3. Digital PID controller, implemented as finite difference equation description of an IIR filter
4. LUT for frequency tuning word association, since modulation steepness is not required to change in real time \rightarrow memory file generated with Matlab script ($f_0, f_{clk}, k_{FM}, n_{bit}^{ADC}, n_{bit}^{FTW}$)



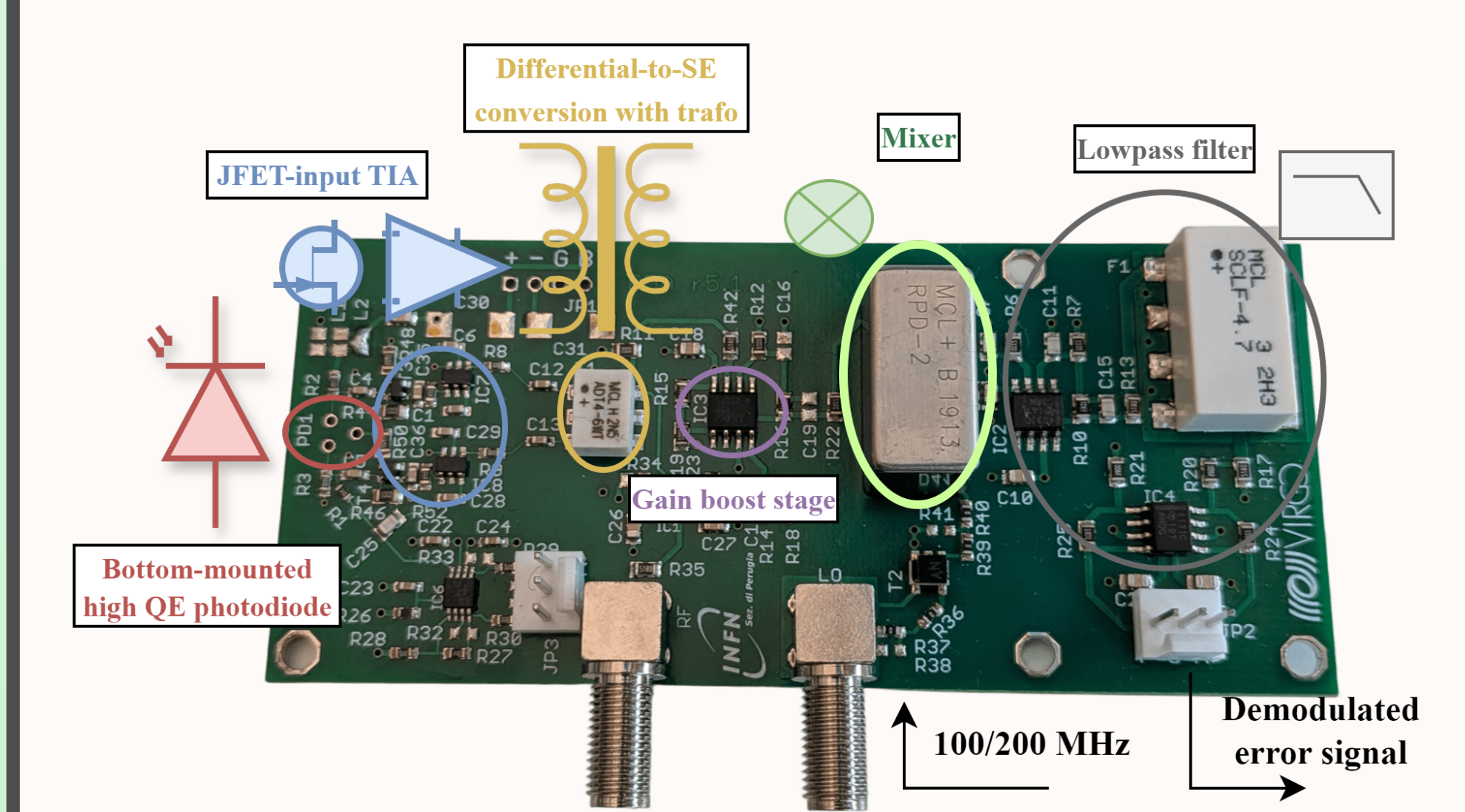
Hardware platform: KCU105 acceleration board \Rightarrow pmod & FMC interfaces used

- Simple circuit: no issues with timing closure @ 100 MHz, few resources;
- KCU105 logical levels (2.5 V) are fully compatible with AD9914 (3.3 V), no level translator needed for board-to-board communication (through FMC to strip cable);
- After initial AD9914 registers configuration, switching to “full-frequency” mode;



- Bottleneck given by ADC’s acquisition rate ($1/t_{acq}$);
 - Tradeoff with resolution (quantization noise);
- 16-bit ADC fully exploits DDS granularity for typical $k_{FM} = 10$ kHz/V
- t_{AOM} & t_{DDS} are fixed;
 - $t_{acq} \sim t_{PID}$ of original setup;
- Additional processing impacts minimally on loop bandwidth, being t_{DDS} (settling time) the limiting factor.

Photodetector front-end

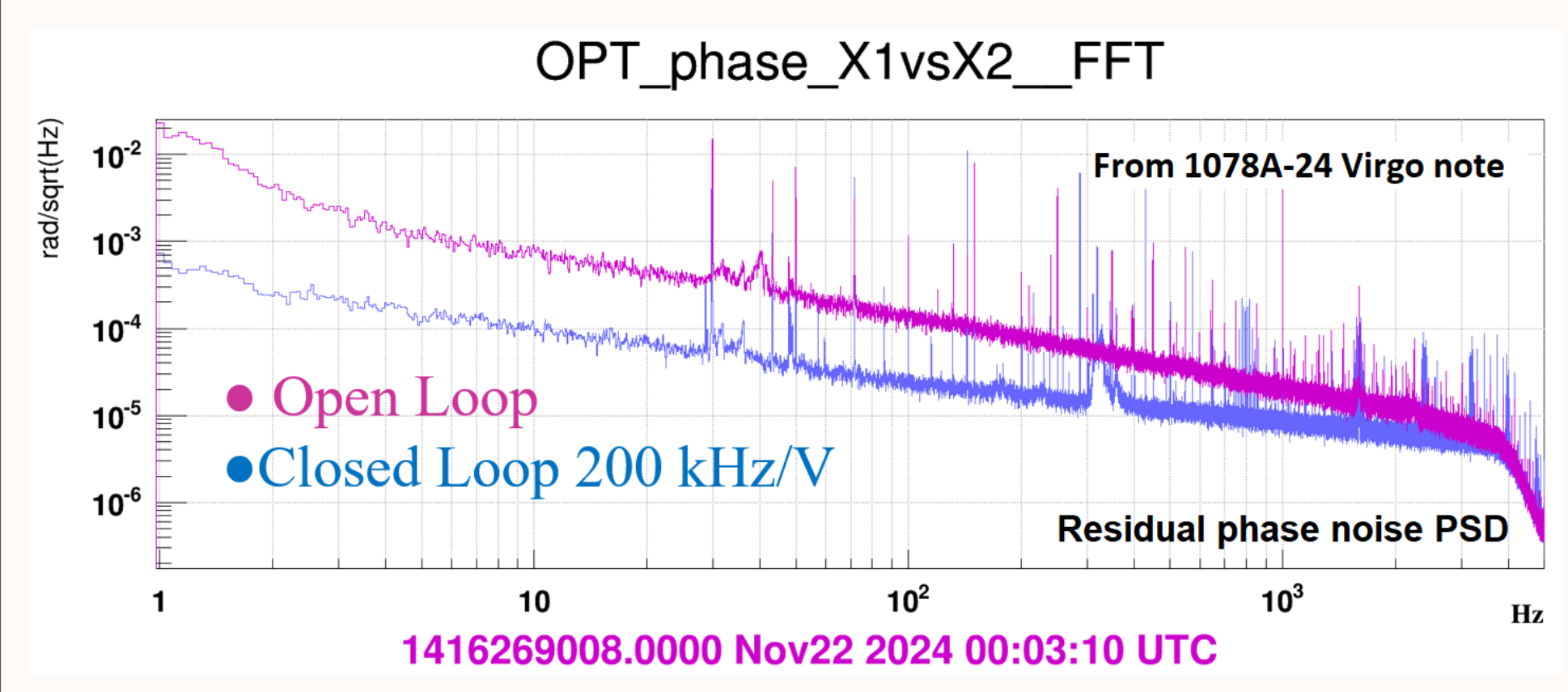


- \rightarrow Differential reading of diode’s photocurrent
- \rightarrow Wideband, low noise amplification
- \rightarrow Demodulation @ f_{LO} and error signal extraction

Loop performance

The optical loop almost behaves like a pure integrator. PID tuning gains were found by applying Ziegler-Nichols method with the loop closed: K_p slowly increased to K_{osc} until constant-amplitude oscillation with period T_{osc} .

$$K_p \approx 0.6 K_{osc}, K_i \approx 1.2 \frac{K_{osc}}{T_{osc}}, T_d \approx 0.125 K_{osc} T_{osc}$$



Further improvements

- Directly apply correction in phase control mode (POW)
- Controller optimization with discrete-time system model
- Introduce ADC and DDS with faster settling

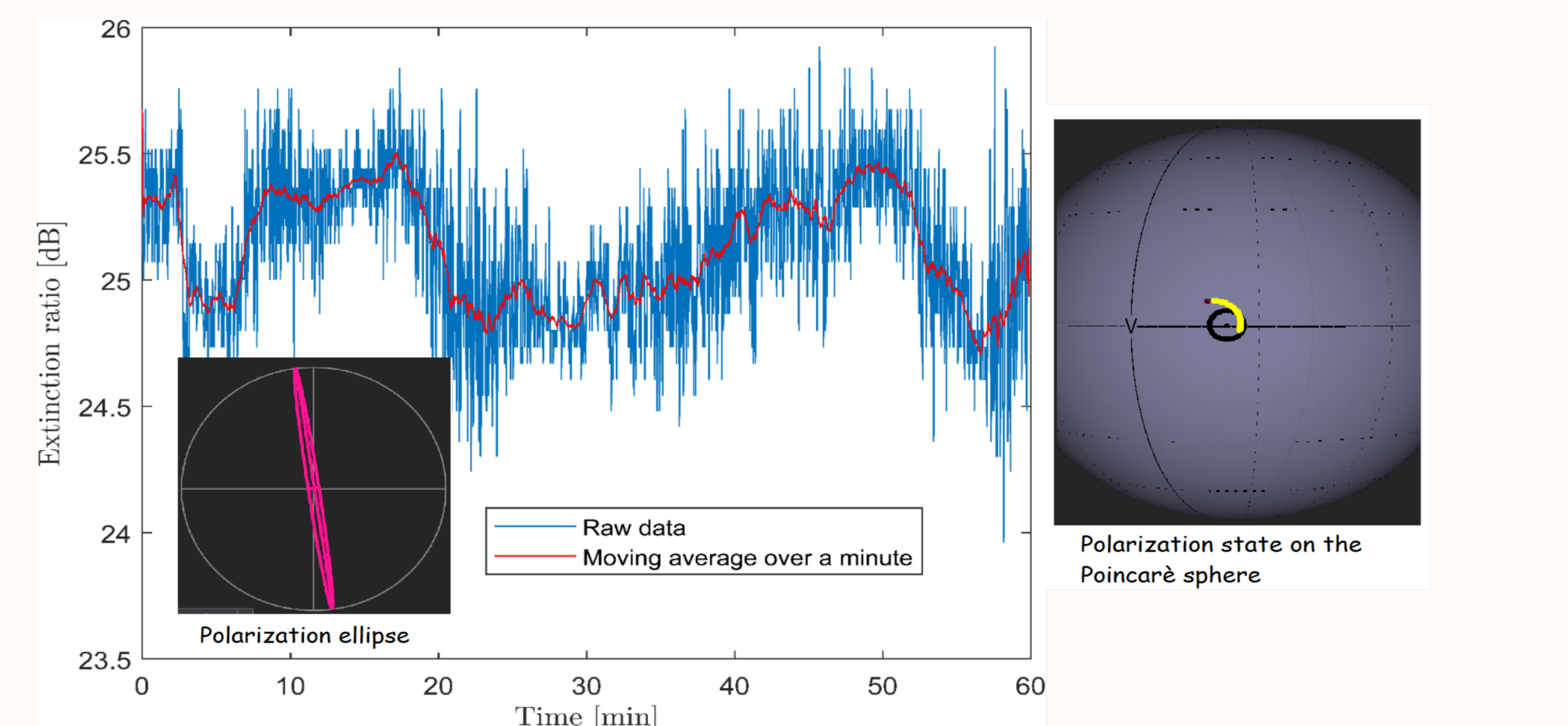
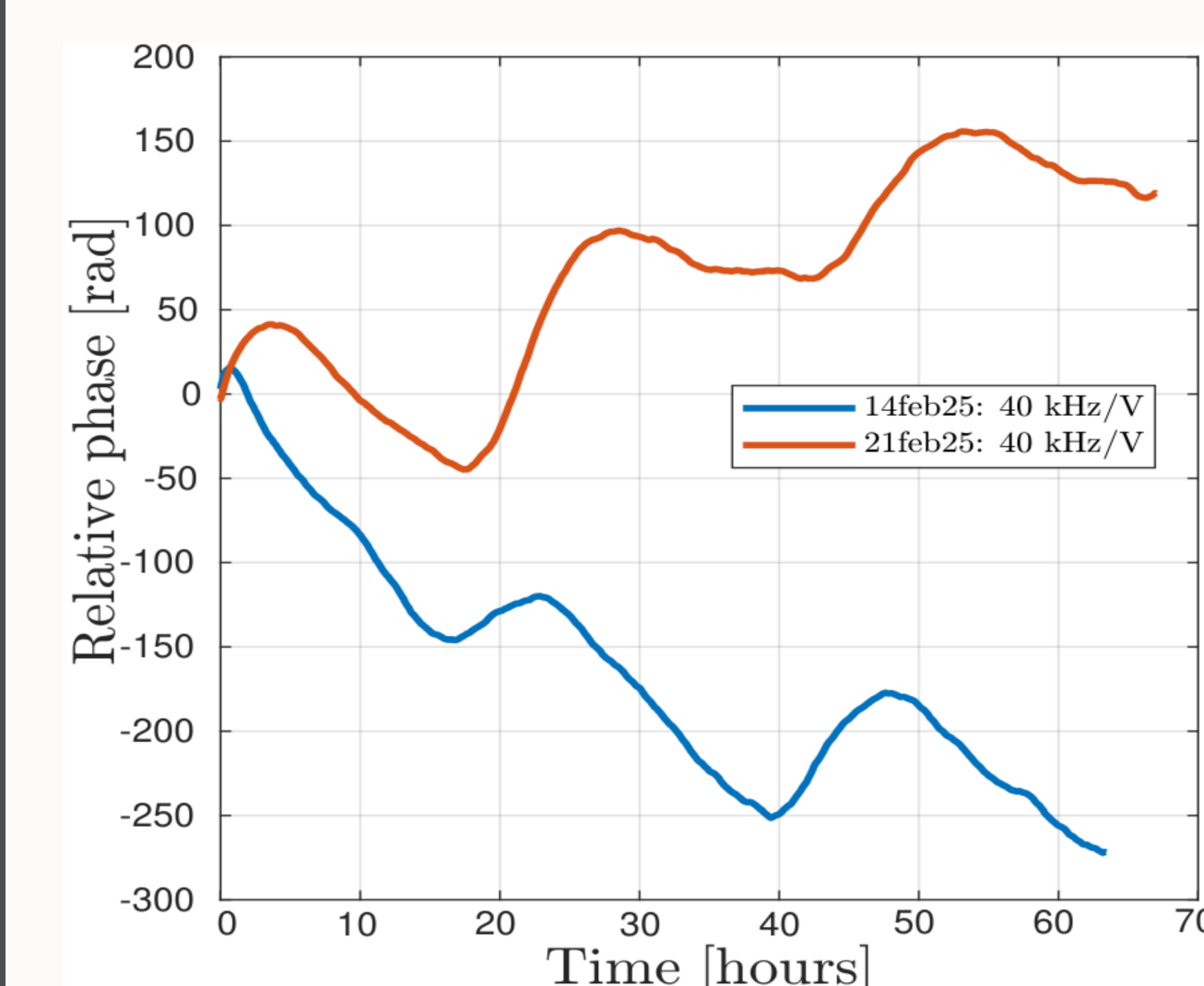
Acknowledgments

Many thanks to M. Giarin of INFN Padova’s mechanical workshop for crafting the new fiberbox, as well as M. Bawaj of INFN Perugia for the design and realization of photodetector electronics.

Environmental effects

Long-term phase monitoring reveals a slow phase wander escaping the effect of feedback. Spectral analysis shows a $1/f^4$ phase noise trend, which indicates some issue of environmental origin. The Allan variance of the time-tagged demodulated tone confirms this suspect, showing a linear trend with observation time τ . Day-night cyclicity has been mitigated by:

1. Placing optical elements & electronic boards far apart;
2. Improve thermal stability of RF circuitry using $2.4 \text{ Wm}^{-1}\text{K}^{-1}$ gapfiller



Changes in the polarization state of fibre-confined light also adds uncertainty to optical phase sensing. Residual ellipticity was minimized using a $\lambda/4$ plate: measured extinction ratio under intense thermal stress (85°C hot-air gun) hits the manufacturing limit of the employed polarization-maintaining (PM) fibers.

References

- [1] C. E. Calosso et al. *Phase noise and amplitude noise in DDS*. In *IEEE International Frequency Control Symposium Proceedings*, 2012.
- [2] Pete Symons. *Digital Waveform Generation*. Cambridge University Press, 2013.
- [3] Enrico Rubiola and François Vernotte. The companion of enrico’s chart for phase noise and two-sample variances. *IEEE Transactions on Microwave Theory and Techniques*, 71(7):2996–3025, July 2023.
- [4] G.F. Franklin, J.D. Powell, and A. Emami-Naeini. *Feedback Control of Dynamic Systems*. Pearson Prentice Hall, 2006.
- [5] Analog Devices. *AD9914 Datasheet*. Technical report, 2022.
- [6] Stanford Research Systems. *SIM960 Operation and service manual*. Technical report, 2013.